BALLISTIC IMPACT MODELING OF COMPOSITE MATERIALS

Chian-Fong Yen
Materials Sciences Corporation
500 Office Center Drive
Fort Washington, PA 19034
(215) 542-8400
yen@materials_sciences.com

Keywords: Ballistic Impact, Composite Materials, Damage Mechanics, Material Model, Rate Effect

ABSTRACT

A computational constitutive model has been developed to characterize the progressive failure behaviors of composite laminates under high velocity ballistic impact conditions. The composite failure model has been implemented within LS-DYNA as a regular material subroutine. The integrated code was successfully utilized to predict the damage and ballistic behavior of composite laminates subjected to various ballistic impact conditions. The availability of this design tool will greatly facilitate the development of composite structures with enhanced ballistic survivability.

INTRODUCTION

Failure modeling of composite materials under impact loading has been the subject of numerous studies, e.g., Abrate (1994), Richarson and Wisheart (1996), Choi and Chang (1990) and Davies and Zhang (1995). However, few studies have been reported on modeling progressive failure in composites under high strain rate ballistic loading. In this work, a rate dependent progressive failure model has been developed to account for the nonlinear and rate dependent behavior commonly observed for fiber reinforced composite materials under high strain rate conditions.

The composite failure model adopted within LS-DYNA is the Chang-Change (1987) model (MAT 22), which provides various fiber and matrix failure modes solely due to in-plane stresses in unidirectional lamina. In this 2D failure model, the failure mode due to out-of-plane shear and normal stresses are neglected. While this may be sufficient for composite structures under in-plane loading, this model may be unable to capture transverse impact failures for which all six stress components are known to contribute to damage development.

To enhance the modeling capability of the progressive failure behavior of composite laminates due to transverse impact, a composite lamina model based on the 3D stress field has been developed by Materials Sciences Corporation (MSC). It has been implemented into LS-DYNA as MAT 161. This failure model can be used to effectively simulate fiber failure, matrix damage, and delamination behavior under all conditions - opening, closure, and sliding of failure surfaces. Furthermore, this progressive failure modeling approach is advantageous as it enables one to predict delamination when locations of delamination sites cannot be anticipated; i.e., locations of potential delamination initiation is calculated without a-priori definition of an interlaminar crack surface. This failure model has been successfully utilized to characterize the impact damage in composite structures for a wide range of impact problems (Yen, et al., 1998a, 1998b, 1999).

In this work, the MSC lamina failure model for fabric composites has been extended to model the progressive post-failure behavior by adopting the continuum damage mechanics approach, which characterizes the growth of damage by decreasing the material stiffness. A continuum damage mechanics (CDM) model for unidirectional composite layers based on plane-stress state was reported by Matzenmiller, et al., (1995). Recent studies reported by William and Vaziri (1995) and VAN HOOF, et al., (1998) have shown that post-failure models of CDM can significantly improve the prediction of impact damage of composite structures. Note that non-interactive failure criteria (based on maximum strain assumption) due to tension, punch shear and crush loading are provided by VAN HOOF, et al., (1998) to account for the major failure modes of ballistic impact of composite materials. This model, however, neglects the rate dependent effect.

High strain rate and high pressure loading conditions generally occur in the impact area when a composite material is subjected to high velocity ballistic impact. Experimental characterization of the mechanical behavior of composite materials under high strain rate conditions has been reported in literature (e.g., Harding and Ruiz 1998 and Al-Hassani and Kaddour 1998). It has been shown that some armor materials such as woven glass and aramid composites exhibit significant rate sensitivity (Harding 1979 and Welsh and Harding 1985). In order to account for the experimentally observed nonlinear and rate dependent behavior, a general rate dependent progressive failure model for a fabric lamina has been developed using the CDM approach provided by Matzenmiller, et al., (1995). The failure criteria and the associated property degradation models are described as follows.

COMPOSITE PROGRESSIVE FAILURE MODEL

Failure models based on the 3D strains in a composite layer with improved progressive failure modeling capability are established for a plain weave fabric layer. It can be used to effectively simulate the fiber failure and delamination behavior under high strain-rate and high pressure ballistic impact conditions. This 3D composite failure model has been successfully integrated into LS-DYNA.

The fabric failure criteria are expressed in terms of ply level engineering strains $\left(\varepsilon_x, \varepsilon_y, \varepsilon_z, \varepsilon_{xy}, \varepsilon_{yz}, \varepsilon_{zx}\right)$ with x, y and z denoting the in-plane fill, in-plane warp and out-of-plane directions, respectively. The associated elastic moduli are $\left(E_x, E_y, E_z, G_{xy}, G_{yz}, G_{zx}\right)$.

Lamina Damage Functions

The fiber failure criteria of Hashin for a unidirectional layer are generalized to characterize the fiber damage in terms of strain components for a plain weave layer. The fill and warp fiber tensile/shear damage are given by the quadratic interaction between the associated axial and through the thickness shear strains, i.e.,

$$f_1 - r_1^2 = \left(\frac{E_x \langle \varepsilon_x \rangle}{S_{xT}} \right)^2 + \left(\frac{G_{xz} \varepsilon_{xz}}{S_{xFS}} \right)^2 - r_1^2 = 0 \qquad (1)$$

$$f_2 - r_2^2 = \left(\frac{E_y \langle \varepsilon_y \rangle}{S_{yT}} \right)^2 + \left(\frac{G_{yz} \varepsilon_{yz}}{S_{yFS}} \right)^2 - r_2^2 = 0$$

where $\langle\ \rangle$ are Macaulay brackets, S_{xT} and S_{yT} are the axial tensile strengths in the fill and warp directions, respectively, and S_{xFS} and S_{yFS} are the layer shear strengths due to fiber shear failure in the fill and warp directions. These failure criteria are applicable when the associated ε_x or ε_y is positive. In equation (1), r_1 and r_2 are the damage thresholds which are equal to 1 without damage.

When ε_x or ε_y is compressive, it is assumed that the in-plane compressive damage in the fill and warp directions are given by the maximum strain criterion, i.e.,

$$f_3 - r_3^2 = \left[\frac{E_x \langle \varepsilon_x' \rangle}{S_{xC}} \right]^2 - r_3^2 = 0, \quad \varepsilon_x' = -\varepsilon_x - \langle -\varepsilon_z \rangle \frac{E_z}{E_x}$$

$$f_4 - r_4^2 = \left[\frac{E_y \langle \varepsilon_y' \rangle}{S_{yC}} \right]^2 - r_4^2 = 0, \quad \varepsilon_y' = -\varepsilon_y - \langle -\varepsilon_z \rangle \frac{E_z}{E_y} \qquad (2)$$

where S_{xC} and S_{yC} are the axial compressive strengths in the fill and warp directions, respectively, and r_3 and r_4 are the corresponding damage thresholds. Note that the effect of through the thickness compressive strain on the in-plane compressive damage is taken into account in equation (2).

When a composite material subjected to transverse impact by a projectile, high compressive stresses will generally occur in the impact area with high shear stresses in the surrounding area between the projectile and the target material. While the fiber shear punch damage due to the high shear stresses can be accounted for by equation (1), the crush damage due to the high through the thickness compressive pressure is modeled using the following criterion:

$$f_5 - r_5^2 = \left(\frac{E_z \langle \varepsilon_z \rangle}{S_{FC}} \right)^2 - r_5^2 = 0 \qquad (3)$$

where S_{FC} is the fiber crush strengths and r_5 is the associated damage thresholds.

A plain weave layer can be damaged under in-plane shear stressing without occurrence of fiber breakage. This in-plane matrix damage mode is given by

$$f_6 - r_6^2 = \left(\frac{G_{xy}\varepsilon_{xy}}{S_{xy}} \right)^2 - r_6^2 = 0 \tag{4}$$

where S_{xy} is the layer shear strength due to matrix shear failure and r_6 is the damage threshold.

Another failure mode, which is due to the quadratic interaction between the thickness stresses, is expected to be mainly a matrix failure. This through the thickness matrix failure criterion is assumed to have the following form:

$$f_7 - r_7^2 = S^2 \left\{ \left(\frac{E_z \langle \varepsilon_z \rangle}{S_{zT}} \right)^2 + \left(\frac{G_{yz}\varepsilon_{yz}}{S_{yz0} + S_{SR}} \right)^2 + \left(\frac{G_{zx}\varepsilon_{zx}}{S_{zx0} + S_{SR}} \right)^2 \right\} - r_7^2 = 0 \tag{5}$$

where r_7 is the damage threshold, S_{zT} is the through the thickness tensile strength, and S_{yz0} and S_{zx0} are the shear strengths for tensile ε_z. The damage surface due to equation (5) is parallel to the composite layering plane. Under compressive through the thickness strain, $\varepsilon_z < 0$, the damaged surface (delamination) is considered to be "closed", and the damage strengths are assumed to depend on the compressive normal strain ε_z similar to the Coulomb-Mohr theory, i.e.,

$$S_{SR} = E_z \tan\varphi \langle -\varepsilon_z \rangle \tag{6}$$

where φ is the Coulomb's friction angle.

When damage predicted by this criterion occurs within elements that are adjacent to the ply interface, the failure plane is expected to be parallel to the layering planes, and, thus, can be referred to as the delamination mode. Note that a scale factor S is introduced to provide better correlation of delamination area with experiments. The scale factor S can be determined by fitting the analytical prediction to experimental data for the delamination area.

Damage Progression Criteria

A set of damage variables ω_i with i = 1, …6, are introduced to relate the onset and growth of damage to stiffness losses in the material. The compliance matrix S is related to the damage variables as (Matzenmiller, et al., 1995):

$$[S] = \begin{bmatrix} \frac{1}{(1-\varpi_1)E_x} & \frac{-\nu_{yx}}{E_y} & \frac{-\nu_{zx}}{E_z} & 0 & 0 & 0 \\ \frac{-\nu_{xy}}{E_x} & \frac{1}{(1-\varpi_2)E_y} & \frac{-\nu_{zy}}{E_z} & 0 & 0 & 0 \\ \frac{-\nu_{xz}}{E_x} & \frac{-\nu_{yz}}{E_y} & \frac{1}{(1-\varpi_3)E_z} & 0 & 0 & 0 \\ 0 & 0 & 0 & \frac{1}{(1-\varpi_4)G_{xy}} & 0 & 0 \\ 0 & 0 & 0 & 0 & \frac{1}{(1-\varpi_5)G_{yz}} & 0 \\ 0 & 0 & 0 & 0 & 0 & \frac{1}{(1-\varpi_6)G_{zx}} \end{bmatrix} \tag{7}$$

The stiffness matrix C is obtained by inverting the compliance matrix, $[C] = [S]^{-1}$.

As suggested in Matzenmiller, et al., (1995), the growth rate of damage variables, $\dot{\varpi}_i$, is governed by the damage rule of the form

$$\dot{\varpi}_i = \sum_j \phi_j q_{ij} \tag{8}$$

where the scalar functions ϕ_i (i=1,…6) control the amount of growth and the vector-valued functions q_{ij} (i=1,…6, j=1,…7) provide the coupling between the individual damage variables (i) in the various damage modes (j). The damage criteria $f_i - r_i^2 = 0$ of equations (1 – 5) provide the damage surfaces in strain space. Damage growth, $\phi_i > 0$, will occur when the strain path crosses the updated damage surface $f_i - r_i^2 = 0$ and the strain increment has a non-zero component in the direction of the normal to the damage surface, i.e., $\sum_j \frac{\partial f_i}{\partial \varepsilon_j}\dot{\varepsilon}_j > 0$. Combined with a damage growth function $\gamma_i\left(\varepsilon_j, \varpi_j\right), j = 1,...6$, ϕ_i is assumed to have the form

$$\phi_i = \sum_j \gamma_i \frac{\partial f_i}{\partial \varepsilon_j}\dot{\varepsilon}_j \quad (no\ sumation\ over\ i) \tag{9}$$

Choosing

$$\gamma_i = \frac{1}{2}\left(1-\varpi_i\right) f_i^{\frac{m}{2}-1} \tag{10}$$

and noting that

$$\sum_j \frac{\partial f_i}{\partial \varepsilon_j}\dot{\varepsilon}_j = \dot{f}_i \tag{11}$$

for the quadratic functions of equations (A1) to (A5), lead to

$$\phi_i = \frac{1}{2}\left(1-\varpi_i\right) f_i^{\frac{m}{2}-1}\dot{f}_i \quad (no\ summation\ over\ i) \tag{12}$$

where ϖ_i' is the damage variable associated with the ith failure mode, and m is a material constant.

For the fiber tensile/shear and compressive damage of modes 1 to 4, the damage coupling vector q_{1i} , q_{2i}, q_{3i} and q_{4i} are chosen such that the fiber damage in either the fill and warp direction results in stiffness reduction in the loading direction and in the related shear directions. For the fiber crush damage of mode 5, the damage coupling vector q_{5i} is chosen such that all the stiffness values are reduced as an element is failed under the crush mode. For the in-plane matrix shear failure of mode 6, the stiffness reduction due to q_{6i} is limited to in-plane shear modulus, while the through the thickness matrix damage (delamination) of mode 7, the coupling vector q_{7i} is chosen for the through thickness tensile modulus and shear moduli. The damage coupling functions q_{ij} are then

$$[q] = \begin{bmatrix} 1 & 0 & 1 & 0 & 1 & 0 & 0 \\ 0 & 1 & 0 & 1 & 1 & 0 & 0 \\ 0 & 0 & 0 & 0 & 1 & 0 & 0 \\ 1 & 1 & 1 & 1 & 1 & 1 & 0 \\ 0 & 0 & 1 & 1 & 1 & 0 & 1 \\ 1 & 1 & 0 & 0 & 1 & 0 & 1 \end{bmatrix} \tag{13}$$

Utilizing the damage coupling functions of equation (13) and the growth function of equation (12), a damage variable ϖ_i can be obtained from equation (8) for an individual failure mode j as

$$\varpi_i = 1 - e^{\frac{1}{m}\left(1 - r_j^m\right)}, \quad r_j \geq 1 \tag{14}$$

Note that the damage thresholds r_i given in the damage criteria of equations (1 – 5) are continuously increasing functions with increasing damage. The damage thresholds have an initial value of one, which results in a zero value for the associated damage variable ϖ_i from equation (14). This provides an initial elastic region bounded by the damage functions in strain space. The nonlinear response is modeled by loading on the damage surfaces to cause damage growth with increasing damage thresholds and the values of damage variables ϖ_i. After damage initiated, the progressive damage model assumes linear elastic response within the part of strain space bounded by the updated damage thresholds. The elastic response is governed by the reduced stiffness matrix associated with the updated damage variables ϖ_i given in equation (7).

When fiber tensile/shear damage is predicted in a layer by equation (1), the load carrying capacity of that layer in the associated direction is reduced to zero according to damage variable equation (14). For compressive fiber damage due to equation (2), the layer is assumed to carry a residual axial load in the damaged direction. The damage variables of equation (14) for the compressive modes have been modified to account for the residual strengths of S_{xCR} and S_{yCR} in the fill and warp directions, respectively, as reported in Yen and Caiazzo (2001).

Figure 1 shows typical axial tensile and compressive stress-strain curves obtained from the damage model. Under monotonic loading, Figure 1a shows that the model provides an initial elastic region up to the strength values (85 ksi for tension and 50 ksi for compression) and a softening region after damage initiated (using a damage parameter m=4). Note that the compressive stress reduces to a residual strength of 15 ksi and remains constant for continuous compressive loading. Figure 1b shows stress-strain curves due to cyclic loading along the axial direction x. It demonstrates the effect of damage history on the stress-strain response. Note that the unloading and reloading stress-strain curves within the damage surface follow the reduced elastic modulus, which is given by the updated damage parameter for the axial fiber damage mode.

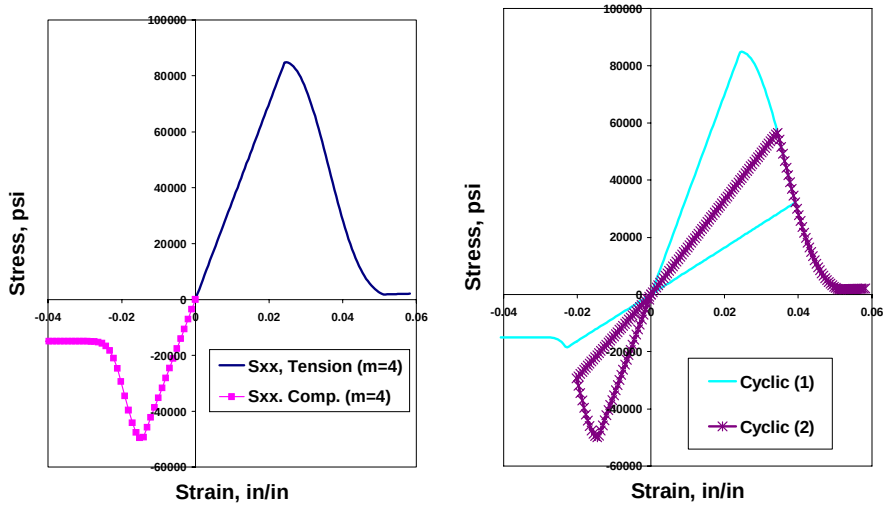

(a) (b)

Figure 1. Axial Stress-Strain Curves for Damage Model Under
(a) Monotonic and (b) Cyclic Loading Conditions

For through the thickness matrix (delamination) failure given by equation (5), the in-plane load carrying capacity within the element is assumed to be elastic (i.e., no in-plane damage). The load carrying behavior in the through the thickness direction is assumed to depend on the opening or closing of the matrix damage surface. For tensile mode, $\varepsilon_z > 0$, the through the thickness stress components are softened and reduced to zero due to the damage criteria described above. For compressive mode, $\varepsilon_z < 0$, the damage surface is considered to be closed, and thus, σ_z is assumed to be elastic, while τ_{yz} and τ_{zx} are allowed to reduce to a sliding friction stress of equation (6). Accordingly, for the through the

thickness matrix failure of mode 7 under compressive mode, the damage variable equation is further modified to account for the residual sliding strength S_{SR} in Yen and Caiazzo (2001).

Figure 2 shows typical axial shear stress-strain curves obtained from the damage model. Shown in Figure 2a are the shear stress-strain curves for τ_{zx} with tensile through the thickness normal loads (opening delamination). Figure 2b shows the effect of the compressive through the thickness normal stress (closing delamination), σ_z on the τ_{zx} stress-strain response for a Coulomb's friction angle $\varphi = 20^0$.

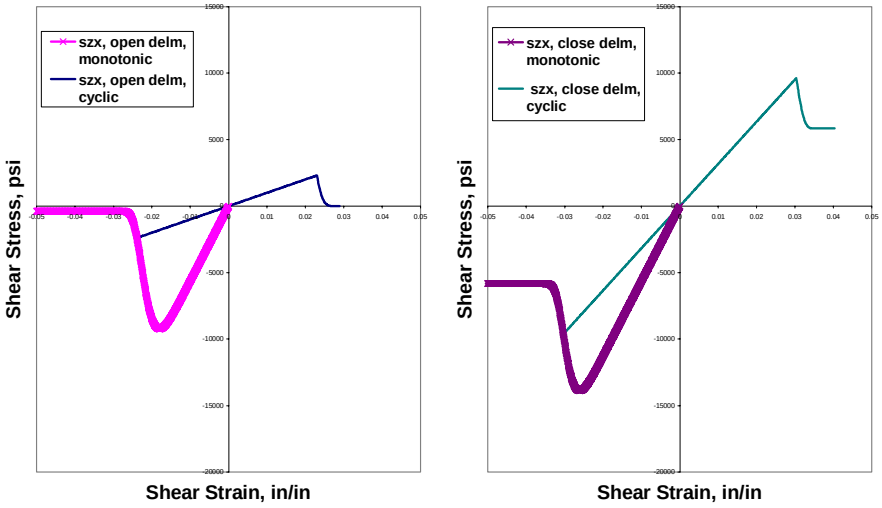

(a) (b)

Figure 2. Shear Stress-Strain Curves for Damage Model under the Effect of Through the Thickness Normal Load, (a) Opening Delamination and (b) Closing Delamination

The effect of strain rate on the layer strength values of the fiber failure modes is modeled by multiplying the associated strength values $\{S_{RT}\}$ by a scale factor as

$$\{S_{RT}\} = \{S_0\}\left(1 + C_{rate} \ln \frac{\{\dot{\varepsilon}\}}{\dot{\varepsilon}_0}\right)$$

$$\{S_{RT}\} = \begin{Bmatrix} S_{xT} \\ S_{yT} \\ S_{xC} \\ S_{yC} \\ S_{FC} \\ S_{xFS} \\ S_{yFS} \end{Bmatrix} \quad and \quad \{\dot{\varepsilon}\} = \begin{Bmatrix} |\dot{\varepsilon}_x| \\ |\dot{\varepsilon}_y| \\ |\dot{\varepsilon}_x| \\ |\dot{\varepsilon}_y| \\ |\dot{\varepsilon}_z| \\ |\dot{\varepsilon}_{zx}| \\ |\dot{\varepsilon}_{yz}| \end{Bmatrix} \tag{15}$$

where C_{rate} is the strain rate constant, and $\{S_0\}$ are the available strength values of $\{S_{RT}\}$ at the reference strain rate $\dot{\varepsilon}_0 = 1s^{-1}$. The effect of strain rate on the axial stress-strain response is shown in Figure 3 for C_{rate}=0.02.

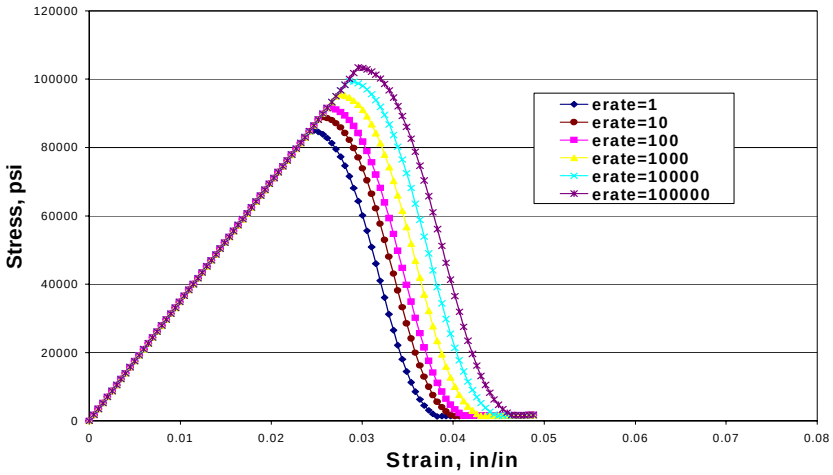

Figure 3. Axial Tensile Stress-Strain Curves for Damage Model Under Various Constant Strain Rate Loading

The functionality of eroding elements is available within the material subroutine by passing in and out some erosion variables. The erosion criterion is formulated by using the fiber tensile failure criterion, equation (1). When fiber tensile failure in both axial directions is predicted in an element, the erosion variables are properly set and passed to LS-DYNA for eliminating the element. The element erosion is necessary in order to avoid the excess distortion of a failed element.

BALLISTIC IMPACT SIMULATION

Simulations of the ballistic impact of two S2-Glass/Epoxy composite panels were conducted by taking account for the strain-rate sensitivity properties. The analyzed ballistic problems were: (1) a 7 psf composite plate subjected to 0.50 caliber FSP impact (Yen and Caiazzo, 2001), and (2) a 4.55 psf composite plate subjected to 0.22 caliber FSP impact. The ballistic analyses were conducted using LS-DYNA integrated with the proposed composite progressive failure model.

The finite element models for the 4.55 psf composite panel and the 0.22 FSP are shown in Figure 4. Only one quadrant of the impact system was modeled due to the geometric and material symmetry. Both the plate and the projectile were modeled with 8-node brick elements with single integration point. There were 24 layers of elements through the thickness.

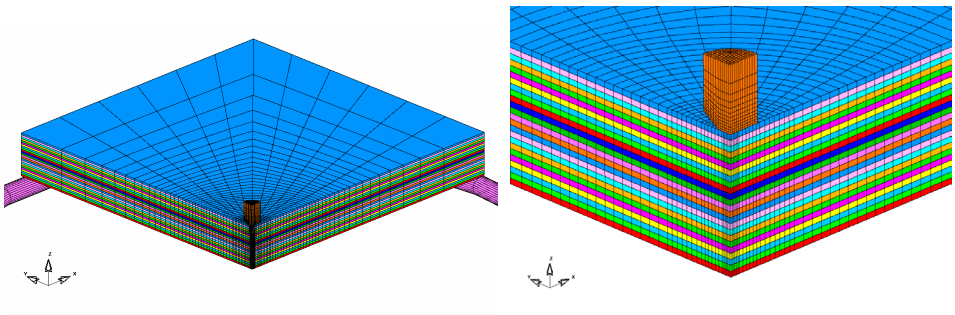

(a) (b)

Figure 4. Finite Element Model for a Composite Panel and a FSP Impactor, (a) Full View, and (b) Close-up of Impact Area

The panel was placed over a rigid ring with a rigid body contact surface assumed between the plate and the ring. Initial velocity was provided to the impactor to start the analysis, the projectile metals were assumed to behave as elastoplastic materials. An eroding contact algorithm provided within LS-DYNA together with the integrated failure model were used to simulate the contact and penetration between the projectile and the impact area of the plate. The element erosion criterion was given by the fiber failure. All failed elements were deleted and the contact surfaces were automatically updated to the next layer of material.

The material properties for an S2-Glass/Epoxy plain weave composite layer and the steel FSP listed in Table 1 were used to perform the simulation. The elastic composite material properties were estimated from the quasi-static properties of the unidirectional S2-glass/Epoxy composite reported in MIL-HDBK-17-3E. Note that the composite layer strengths related to the fiber failure, which include the in-plane tensile and compressive strengths as well as the out-of-plane punch shear and crush strengths, have strong effects on the composite ballistic behavior. Test data for these strength properties of the plain weave S2-glass/epoxy are currently not available. Due to the lack of test data, the strain rate constant C = 0.1 obtained for a fine weave glass/epoxy woven material reported by Harding (1979) and Welsh and Harding (1985) was used for the current analysis. While the quasi-static tensile strength of 85 ksi and compressive strength of 50 ksi were estimated from those of the unidirectional composite, the quasi-static punch shear strength and compressive crush strength were taken to be 80 ksi and 100 ksi, respectively. The punch shear strength and the crush strength were chosen to provide the best fit to the V50 value of the 7 psf plate subjected to 0.50 FSP impact. This set of material properties were then used to predict the V50 of the 4.55 psf plate subjected to 0.22 FSP impact.

Figure 5 shows the time histories of projectile velocity for three values of initial impact velocity. Note that the initial velocity is negative (downward) and the rebounding velocity is positive (upward). It is seen from Figure 5 that the predicted V50 of the second panel is about 2400 fps, which is about 13% lower than the experimental value of 2775 fps. Figure 6 shows the comparison of the damaged mesh plots and the cross sections of tested panels for the initial impact velocities of 2125 fps and 2924 fps. Figure 6 clearly demonstrates the eroding failure of the composite panel due to the combination of fiber failure modes of punch shear, crush and tension. These results show good correlation of ballistic fiber damage between the computed and tested results.

Table 1. Material Properties Used for Dynamic Analysis

S2-glass/Epoxy Plain Weave Layer

$E_x = E_y$ = 24.1 GPa (3.5 Msi)	E_z = 10.4 GPa (1.51 Msi)
ν_{xy} = 0.12	$\nu_{xz} = \nu_{yz}$ = 0.40
$G_{xy} = G_{yz} = G_{zx}$ = 5.9 GPa (0.85 Msi)	
$S_{xT} = S_{yT}$ = 0.59 GPa (85 ksi)	$S_{xC} = S_{yC}$ = 0.35 GPa (50 ksi)
S_{zT} = 69 MPa (10 ksi)	$S_{FC}{}^{\dagger}$ = 0.69 GPa (100 ksi)
$S_{FS}{}^{\dagger}$ = 0.55 GPa (80 ksi)	$S_{xCR}{}^{\dagger} = S_{yCR}{}^{\dagger}$ = 0.10 GPa (15 ksi)
$S_{xy} = S_{yz} = S_{zx}$ = 48.3 MPa (7 ksi)	
S = 1.4	C = 0.1
$\phi^{\dagger} = 40^0$	$m^{\dagger}$ = 4
ρ = 1783 Kg/m^3 (1.668x10^{-4} lbs-sec^2/in^4)	

Steel 4340

E = 207 GPa (30 Msi)	ν = 0.33
σ_y * = 1.03 GPa (150 Ksi)	E^t ** = 6.9 GPa (1.0 Msi)
ε_f ***= 1.2	ρ = 7877 Kg/m^3 (7.37x10^{-4} lbs-sec^2/in^4)

† Estimated values * Yield stress ** Plastic tangent modulus *** Failure strain

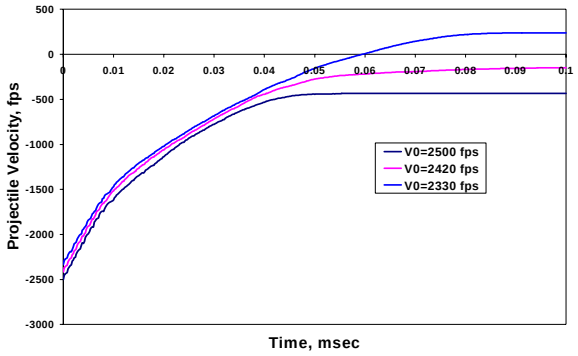

Figure 5. Computed Time Histories of Projectile Velocity for an S2-Glass/Epoxy Composite Subjected to 0.22 Caliber FSP Impact

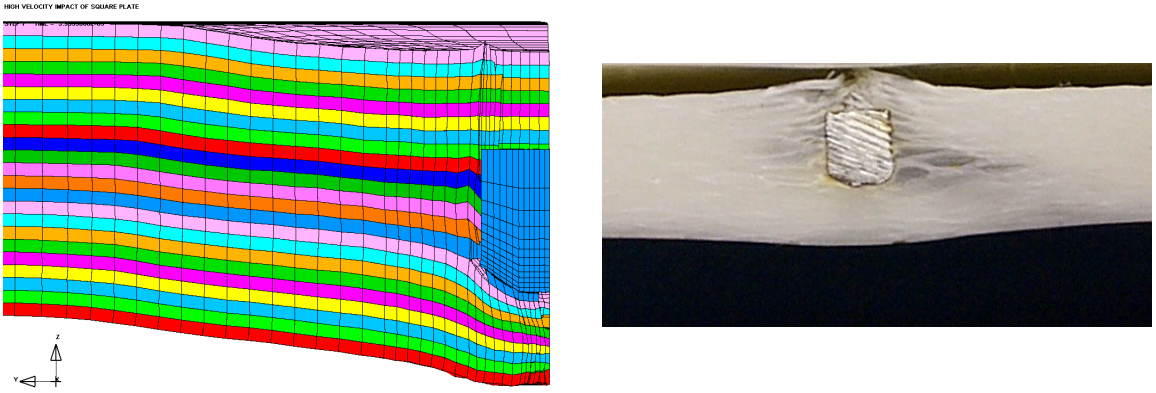

(a)

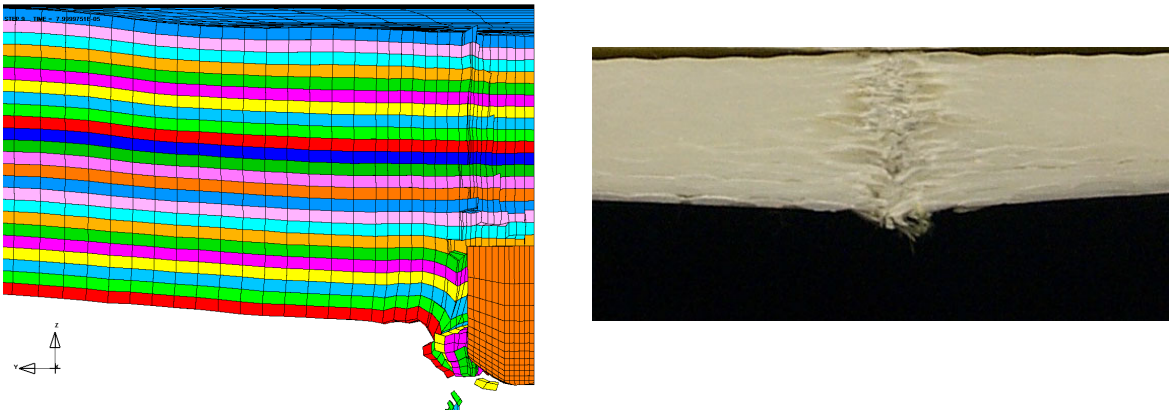

(b)

Figure 6. Comparison of the Finite Element and Experimental Results of Damage 0.55 psf Composite Panel Subjected to 0.22 Cal. FSP Impact at (a) 2125 fps and (b) 2924 fps

CONCLUSIONS

A strain rate dependent lamina model based on CDM has been successfully developed and implemented within LS-DYNA for modeling the progressive failure behavior of plain weave composite layers. It can be used to effectively simulate the fiber failure and delamination behavior under high strain-rate and high-pressure ballistic impact conditions. The integrated code was successfully utilized to predict the ballistic limit velocity of composite laminates subjected to high velocity ballistic impact conditions. Simulations of ballistic impact of composite panels have been conducted by taking account for the strain-rate sensitivity properties. The strain rate effect will need further investigation by experimentally characterizing the rate dependent behavior of various composite materials. Correlation for impact damage such as delamination area will also need to be conducted when the test data is available in the future.

ACKNOWLEDGMENT

This work was supported by the U.S. Army Research Laboratory under Contract No. DAAD17-00-C-0059.

REFERENCES

Abrate, A. (1994). “Impact on Laminated Composites: Recent Advances,” Appl. Mech. Rev., V47, pp. 517-543.

Al-Hassani, S.T.S. and Kaddour, A.S. (1998). “Strain Rate Effects on GRP, KRP and CFRP Composite Laminates,” Key Engineering Materials, Vol. 141-143, Trans Tech Publications, Switzerland, pp. 427-452.

Choi, H.Y., and Chang, F.K. (1990). “Impact Damage Threshold of Laminated Composites”, in Failure Criteria and Analysis in Dynamic Response, AMD Vol. 107, ASME Applied Mechanics Division, Dallas, TX, November 1990, pp. 31-35.

Chang, F.K., and Chang, K.Y. (1987). “A Progressive Damage Model for Laminated Composites Containing Stress Concentration,” J. of Composite Materials, Vol. 21, pp. 834-855.

Davies, G.A.O., and Zhang, X. (1995). “Impact Damage Prediction in Carbon Composite Structures”, Int. J. Impact Engng., Vol. 16, pp. 149-170.

Harding J. (1979). “The High-Speed Punching of Woven-Roving Glass-Reinforced Composites.” Inst. Phys. Conf. Ser. No. 47: Chapter 3, The Institute of Physics, Bristol and New York, pp. 318-330.

Harding, J. and Ruiz, C. (1998). ”The Mechanical Behaviour of Composite Materials under Impact Loading,” Key Engineering Materials, Vol. 141-143, Trans Tech Publications, Switzerland, pp. 403-426.

Matzenmiller, A., Lubliner, J., and Taylor, R.L. (1995). “A Constitutive Model for Anisotropic Damage in Fiber-Composites,” Mechanics of Materials, 20, pp. 125-152.

Richarson, M.O.W., and Wisheart, M.J. (1996). “Review of Low-Velocity Impact Properties of Composite Materials”, Composites, Vol., 27A, pp. 1123-1131.

VAN HOOF, J., WOESWICK, M.J., STRAZNICKY, P.V., BOLDUC, m. AND TYLKO, S.(1998). Proceedings of the 5th International LS-DYNA Users Conference.

Welsh, L.M. and Harding, J. (1985) “Effect of Strain Rate on the Tensile Failure of Woven Reinforced Polyester Resin Composite.” Proc. DYMAT 85, Int. Conf. On Mech. And Physical Behaviour of Materials under Dynamic Loading, Jour de Physique, Colloque C5, pp. 405-414.

William, K. and Vaziri, R., (1995). “Finite Element Analysis of the Impact Response of CFRP Composite Plates.” Proceedings of the ICCM-11, pp. 532-654.

Yen, C.F., Cassin, T., Patterson, J., and Triplett, M. (1998a). “Progressive Failure Analysis of Thin Walled Composite Tubes under Low Energy Impact,” 39th AIAA Structures, Structural Dynamics, and Materials Conference.

Yen, C.F., Cassin, T., Patterson, J., and Triplett, M. (1998b). “Progressive Failure Analysis of Composite Sandwich Panels under Blast Loading,” Structures Under Extreme Loading Conditions, ASME PVP-Vol. 361, New York, pp. 203-216.

Yen, C.F., Cassin, T., Patterson, J., and Triplett, M. (1999). “Analytical Methods for Assessing Impact Damage in Filament Wound Pressure Vessels,” 44th International SAMPE Symposium and Exposition, Long Beach, CA. May 23-27.

Yen, C.F. and Caiazzo, A. (2001). “Innovative Processing of Multifunctional Composite Armor for Ground Vehicles.” ARL-CR-484, U.S. Army Research Laboratory, Aberdeen Proving Ground, MD.